

# Single-parameter aging in a binary Lennard-Jones system

Cite as: J. Chem. Phys. 154, 094504 (2021); doi: 10.1063/5.0039250

Submitted: 1 December 2020 • Accepted: 24 January 2021 •

Published Online: 2 March 2021



View Online



Export Citation



CrossMark

Saeed Mehri,<sup>a)</sup>  Trond S. Ingebrigtsen,<sup>b)</sup>  and Jeppe C. Dyre<sup>b)</sup> 

## AFFILIATIONS

Glass and Time, IMFUFA, Department of Science and Environment, Roskilde University, P.O. Box 260, DK-4000 Roskilde, Denmark

<sup>a)</sup> Author to whom correspondence should be addressed: mehri@ruc.dk

<sup>b)</sup> dyre@ruc.dk

## ABSTRACT

This paper studies physical aging by computer simulations of a 2:1 Kob–Andersen binary Lennard-Jones mixture, a system that is less prone to crystallization than the standard 4:1 composition. Starting from thermal-equilibrium states, the time evolution of the following four quantities is monitored by following up and down jumps in temperature: potential energy, virial, average squared force, and the Laplacian of the potential energy. Despite the fact that significantly larger temperature jumps are studied here than in typical similar experiments, to a good approximation, all four quantities conform to the single-parameter-aging scenario derived and validated for small jumps in experiments [T. Hecksher, N. B. Olsen, and J. C. Dyre, J. Chem. Phys. 142, 241103 (2015)]. As a further confirmation of single-parameter aging with a common material time for the four different quantities monitored, their relaxing parts are found to be almost identical for all temperature jumps.

Published under license by AIP Publishing. <https://doi.org/10.1063/5.0039250>

## I. INTRODUCTION

It is of great interest to be able to predict how much and how fast material properties change over time.<sup>1</sup> Such gradual property changes are referred to as aging. Corrosion and weathering, in general, give rise to aging. The term “physical aging” refers to changes in material properties that result exclusively from molecular rearrangements, i.e., involve no chemical changes.<sup>2–4</sup> A number of theories of physical aging have been developed,<sup>2–15</sup> and physical aging has been the subject of experimental studies in different contexts dealing with, e.g., oxide glasses,<sup>3,4</sup> polymers,<sup>5,16–20</sup> metallic glasses,<sup>21,22</sup> colloids,<sup>22</sup> and spin glasses.<sup>23,24</sup> Examples of quantities monitored in order to probe physical aging are density,<sup>19,25</sup> enthalpy,<sup>3,6</sup> Young’s modulus,<sup>19</sup> and various frequency-dependent responses.<sup>7,8,26–32</sup>

Physical aging is generally both non-exponential and non-linear. The latter property is reflected in the fact that the system’s response to a small perturbation depends on both the sign and the magnitude of the input. Ideally, an aging experiment consists of an up or a down jump in temperature starting from a state of thermal

equilibrium, eventually ending in equilibrium at the “target” (annealing) temperature. The hallmark of aging is that these two responses, even if they go to the same temperature, are *not* mirror symmetric. A down jump is fast at the beginning but slows down gradually as equilibrium is approached (“self-retarding”). An up jump—while slower in the beginning—will, after an initial delay, show a steeper approach to equilibrium (“self-accelerating”).<sup>4,9,19</sup> This is the fictive-temperature effect, also referred to as “asymmetry of approach,”<sup>33–35</sup> an effect that is well understood as a consequence of the fact that the relaxation rate itself ages.<sup>4–6,16,36–39</sup>

In experimental studies of physical aging, the temperature  $T$  is externally controlled and identified as the phonon “bath” temperature measured on a thermometer. Recently, Hecksher *et al.*<sup>8</sup> and Roed *et al.*<sup>40</sup> studied the physical aging of glass-forming liquids around the glass transition temperature by probing the shear-mechanical resonance frequency ( $\sim 360$  kHz), the dielectric loss at 1 Hz, the real part of the dielectric constant at 10 kHz, and the loss-peak frequency of the dielectric beta process ( $\sim 10$  kHz). These authors developed a “single-parameter aging” (SPA) formalism as a simple realization of Narayanaswamy’s idea that a material time

controls aging.<sup>3</sup> SPA basically allows one to predict the normalized relaxation functions of an arbitrary temperature jump from the data of a single jump. SPA was first demonstrated for jumps to the same temperature for three different van der Waals liquids<sup>8</sup> and subsequently generalized to deal with jumps ending at different temperatures in a study of glycerol.<sup>40</sup>

The motivation of this study is to illuminate how general SPA is by investigating whether SPA applies also in computer simulations. The advantage of simulations is that one can probe well-defined microscopic quantities and, for instance, easily study the aging of several different quantities under identical circumstances. We report below data for the physical aging of a binary Lennard-Jones mixture upon a temperature jump. The following four quantities were monitored: virial, potential energy, average squared force, and the Laplacian of the potential energy. We find that all four quantities conform to SPA to a good approximation, even for temperature jumps as large as 10%.

## II. THE TOOL-NARAYANASWAMY MATERIAL-TIME CONCEPT

Above the melting temperature, a liquid is rarely particularly viscous. At lower temperatures, the liquid becomes supercooled, and because of the extraordinary large viscosities reached upon further cooling, the liquid gradually behaves more like a “solid that flows” than like an ordinary liquid.<sup>41</sup> For both the ordinary liquid phase and the glass phase, under ambient pressure conditions, physical properties are found to depend only on the temperature. At temperatures in the vicinity of the glass transition temperature (defined by the applied cooling and heating rates), however, the behavior is different. In this temperature range, the molecular structure changes gradually with temperature, and following an external perturbation, a noticeable delay is observed before equilibrium is reached. In this case, the physical properties depend not just on the actual temperature, but on the entire thermal history of the system.

In 1971, Narayanaswamy established what has become the standard formalism for physical aging. It was developed for predicting how the frozen-in stresses in a wind shield depend on the glass's thermal history during production. The theoretical framework, which turned out to be generally applicable for physical aging involving moderate temperature changes,<sup>3,4</sup> is now referred to as the Tool-Narayanaswamy (TN) formalism. This framework systematically addresses the non-exponential and non-linear nature of aging. The TN formalism reproduces all observed qualitative features of physical aging, and it is also in quantitative agreement with experiments.<sup>2-4,42,43</sup>

The crucial concept of TN is that of a *material time*, denoted by  $\xi$ . The material time may be thought of as the time measured on a clock with a clock rate,  $\gamma(t)$ , that changes as the material ages. Simply put, the material time is the time that a substance “experiences,” which in equilibrium is proportional to the actual time. In this physical picture, one expects the existence of a single material time controlling the physical aging of different quantities.

Since the clock rate by definition measures how fast the material time changes,<sup>3,43</sup> one has

$$d\xi = \gamma(t)dt. \quad (1)$$

Narayanaswamy showed from experimental data that if one switches from time to material time the aging response becomes linear. In other words, a non-linear aging response is described by a *linear* convolution integral over the material time.<sup>3,4</sup> This was an important and highly nontrivial finding. For instance, it implies that the “asymmetry of approach” becomes a “symmetry of approach” when jumps of equal magnitude to the same temperature are considered as functions of the material time.

## III. SIMULATION DETAILS

The simulations were performed in the *NVT* ensemble with the Nosé–Hoover thermostat using the RUMD (Roskilde University Molecular Dynamics) GPU open-source code (<http://rumd.org>). We simulated a system of 10 002 particles consisting of two different Lennard-Jones (LJ) spheres, A and B. Writing the LJ pair potential between particles of type  $\alpha$  and  $\beta$  as  $v_{\alpha\beta}(r) = \epsilon_{\alpha\beta}((r/\sigma_{\alpha\beta})^{-12} - (r/\sigma_{\alpha\beta})^{-6})$  ( $\alpha, \beta = A, B$ ), the parameters used are  $\sigma_{AA} = 1.0$ ,  $\sigma_{AB} = \sigma_{BA} = 0.8$ ,  $\sigma_{BB} = 0.88$ ,  $\epsilon_{AA} = 1.0$ ,  $\epsilon_{AB} = \epsilon_{BA} = 1.5$ , and  $\epsilon_{BB} = 0.5$ . All simulations employed a MD time step of 0.0025 (in the units defined by the A particle parameters) and a shifted-potential cutoff of  $v_{\alpha\beta}(r)$  at  $r_{\text{cut}} = 2.5\sigma_{\alpha\beta}$ . The pair-potential parameters are the same as those of the well-known Kob–Andersen (KA) mixture,<sup>44</sup> which has previously been used for numerical studies of physical aging and other glass-transition related non-equilibrium phenomena.<sup>45-49</sup> We use a ratio of A and B particles that is 2:1 instead of the standard 4:1 ratio, however, because the 2:1 mixture is much more resistant toward crystallization than the 4:1 composition<sup>50-52</sup> (an alternative option for avoiding crystallization of KA mixtures is to keep the 4:1 composition and employ a short-distance shifted-force cutoff for the AA and BB interactions<sup>53</sup>). To facilitate a comparison of results for the two different compositions, we note that the mode-coupling temperature is around 0.55 for the 2:1 KA system, whereas it is around 0.44 for the standard mixture.

All results reported below were obtained at density 1.4 (in A particle units) and represent averaging over 100 simulations. Each data point was obtained by averaging in time every 2048 time steps for an interval of 32 768 time steps. Before performing a temperature jump, the system was carefully equilibrated. To reach equilibrium at the lowest temperature ( $T = 0.50$ ) and ensure that there is no crystallization issue, we first simulated the system by performing  $2.4 \times 10^{11}$  time steps. After this, 100 equilibrium configurations were obtained by dumping a configuration every  $1.678 \times 10^8$  time steps, which is of the same order of magnitude as the average relaxation time. At higher temperatures, equilibrium is reached much faster, of course.

Initially, the following five quantities were probed: the potential energy, the virial, the configurational temperature defined by

$$k_B T_{\text{conf}} = \frac{\langle (\nabla U)^2 \rangle}{\langle \nabla^2 U \rangle}, \quad (2)$$

its numerator (the average squared force), and its denominator (the Laplacian of the potential energy). In equilibrium in the thermodynamic limit, the configurational temperature is equal to the temperature  $T$ . The data of this study, obtained after averaging over 100 simulations, are presented in Figs. 1 and 2. We find that the configurational temperature does not age but equilibrates almost instantaneously [Fig. 1(c)], confirming previous results by

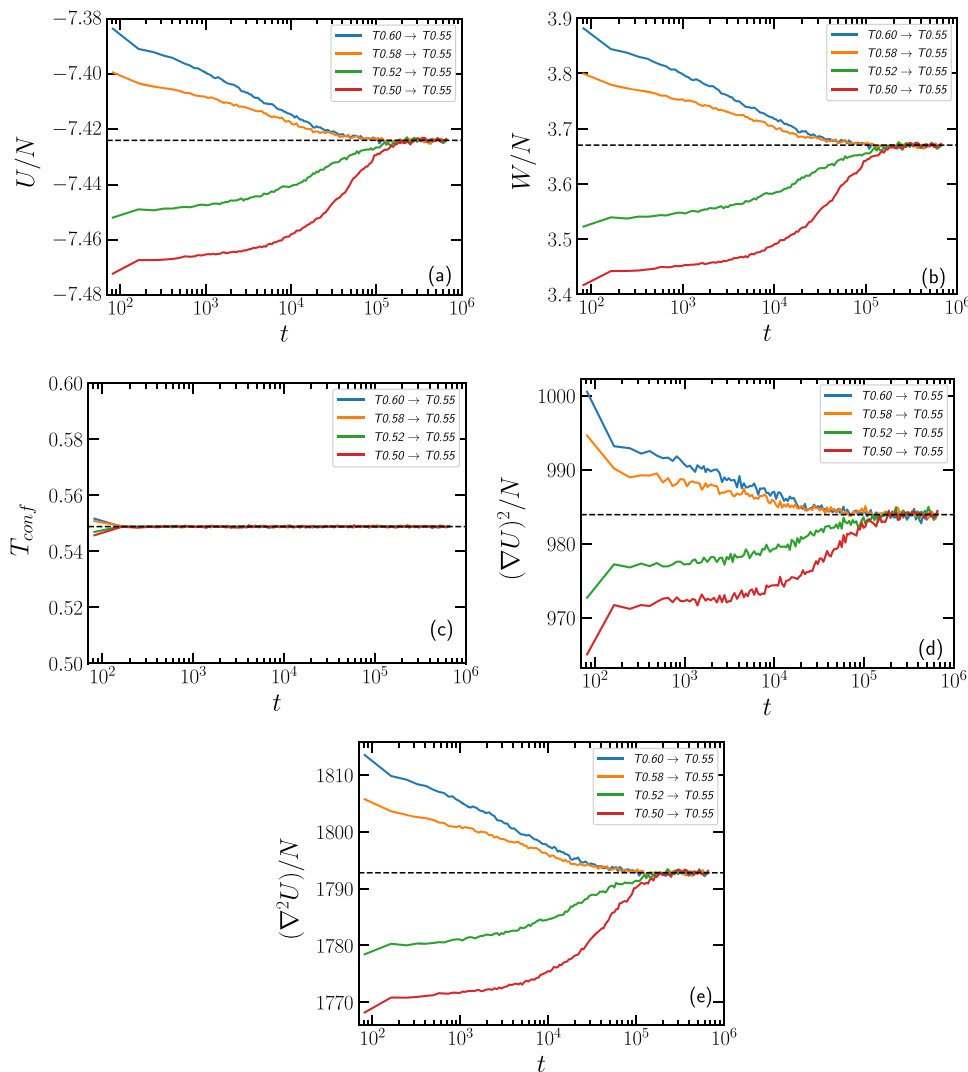


**FIG. 1.** Aging data for jumps to the same target temperature. Each panel shows four jumps from  $T_{\text{start}} = T_0 + \Delta T$  to  $T_0 = 0.55$  with  $\Delta T = \pm 0.03$  and  $\Delta T = \pm 0.05$ . Results for temperature up jumps are shown in red and green, while those for down jumps are shown in blue and orange. The fictive-temperature effect (asymmetry of approach) is clearly observed, with down jumps being faster and more stretched than up jumps: (a) potential energy; (b) virial; (c) configurational temperature [Eq. (2)], which does not age; (d) average squared force; and (e) the Laplacian of the potential energy.

Powles *et al.*<sup>54</sup> We have no simple explanation of this observation. The remainder of the paper focuses on the aging of the four other quantities. These quantities are easily probed and obvious choices for testing SPA in a computer simulation.

After equilibration at each starting temperature  $T_{\text{start}} = T_0 + \Delta T$ , we initiate an aging simulation at  $t = 0$  by changing the thermostat temperature to the “target” temperature  $T_0$ . The system eventually reaches the thermal equilibrium at  $T_0$ . We denote the quantity probed by  $\chi(t)$ . The equilibrium value of  $\chi$  at  $T_0$  is denoted by  $\chi_{\text{eq}}$ , while  $\chi(0)$  is the equilibrium value of  $\chi$  at  $T_{\text{start}}$ , i.e., just before the jump is initiated at  $t = 0$ .

From  $\chi(t)$ , we define for each temperature jump the normalized relaxation function  $R(t)$  by subtracting the value of  $\chi$  at  $T_0$  from the value at each time, subsequently dividing by the overall change, i.e.,

$$R(t) \equiv \frac{\chi(t) - \chi_{\text{eq}}}{\chi(0) - \chi_{\text{eq}}}. \quad (3)$$

Note that while  $R(0) = 1$  just before the jump is initiated, within a few time steps after  $t = 0$  there is a significant “instantaneous” drop in  $R(t)$ . Aging descriptions conventionally focus only on the subsequent, relaxing part of the temperature response, but it is convenient to use instead the above defined  $R(t)$  because this quantity can be determined directly from the data without having to estimate the magnitude of the initial “instantaneous” change of  $\chi$ .

#### IV. SINGLE-PARAMETER AGING

We briefly review here the derivation of SPA, which is based on two assumptions within the TN formalism.<sup>8,40</sup> The first assumption is that the clock rate,  $\gamma(t)$ , is determined by the monitored parameter  $\chi(t)$  itself. The second assumption is that temperature changes are so small that a first-order Taylor expansion of the logarithm of the aging rate in terms of  $\chi$  applies. If  $\Delta\chi(t) \equiv \chi(t) - \chi_{\text{eq}}$  is the variation of

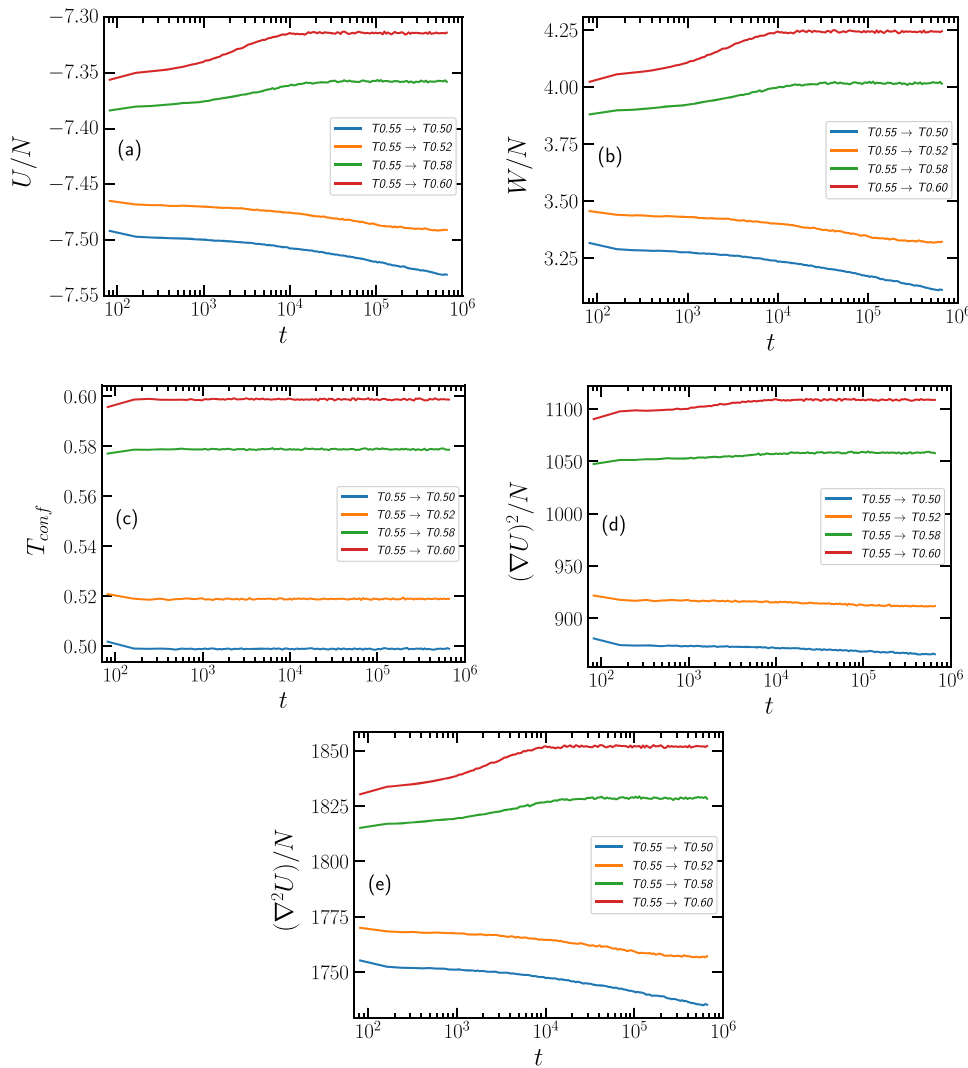


**FIG. 2.** Aging data for jumps from the same temperature. Each panel shows four jumps from  $T_0 = 0.55$  to  $0.55 + \Delta T$  with  $\Delta T = \pm 0.03$  and  $\Delta T = \pm 0.05$ . Results for temperature up jumps are shown in red and green, while those for down jumps are shown in blue and orange. Note that the scale on the y axis is different from that of Fig. 1. (a) Potential energy, (b) virial, (c) configurational temperature, (d) average squared force, and (e) the Laplacian of the potential energy.

$\chi$  from its equilibrium value at the target temperature  $T_0$  [implying that  $\Delta\chi(t) \rightarrow 0$  as  $t \rightarrow \infty$ ], the first-order Taylor expansion leads to<sup>8</sup>

$$\ln \gamma(t) = \ln \gamma_{\text{eq}} + \Delta\chi(t)/\chi_{\text{const}}, \quad (4)$$

in which  $\gamma_{\text{eq}}$  is the equilibrium relaxation rate at the target temperature  $T_0$  and  $\chi_{\text{const}}$  is a constant of the same dimension as  $\chi$ . This expression summarizes the general SPA framework. In conjunction with the TN basic assumption that physical aging is a linear response in the temperature variation when formulated in terms of the material time, SPA may be applied to any relatively small temperature variation, no matter whether it is continuous or discontinuous. We henceforth consider the simplest case with that of a (discontinuous) temperature jump.

Since  $\Delta\chi(t) = \Delta\chi(0)R(t)$  by the definition of  $R(t)$ , Eq. (4) implies<sup>8</sup>

$$\gamma(t) = \gamma_{\text{eq}} \exp\left(\frac{\Delta\chi(0)}{\chi_{\text{const}}} R(t)\right). \quad (5)$$

The normalized relaxation function  $R(t)$  is given by<sup>3,4,8</sup>

$$R(t) = \Phi(\xi). \quad (6)$$

The point of the TN formalism is that the function  $\Phi(\xi)$  is the same for all temperature jumps. In contrast, the time dependence of the material time,  $\xi(t)$ , is not universal because the aging rate changes as the system ages. In conjunction with the definition of the aging rate in terms of the material time [Eq. (1)], Eq. (6) implies  $\dot{R}(t) = \Phi'(\xi)\dot{\xi}(t)$ . Since Eq. (6) means that  $\xi$  is the same function of  $R$  for all jumps, by defining  $F(R) \equiv -\Phi'(\xi(R))$ , one gets<sup>8</sup>

$$\dot{R}(t) = -F(R)\gamma(t). \quad (7)$$

The negative sign in Eq. (7) is convenient because  $R(t)$  is (usually) a monotonically decreasing function of time, thus making  $F(R)$  positive.

Equations (5) and (7) lead to

$$-\frac{\dot{R}(t)}{\gamma_{eq}} \exp\left(-\frac{\Delta\chi(0)}{\chi_{const}} R(t)\right) = F(R(t)). \quad (8)$$

Since the right-hand side for a given value of  $R(t)$  is independent of the jump sign and magnitude, this applies also for the left-hand side. This prediction was validated in 2015 in experiments monitoring four different quantities.<sup>8</sup> From Eq. (8), one can basically predict the relaxation function of one jump from the relaxation function of another jump since a single jump is enough to determine the function  $F(R)$ . In order to determine the constant  $\chi_{const}$ , however, two jumps are needed (see below); alternatively, a determination of the equilibrium relaxation rate at two different temperatures can also be used to find  $\chi_{const}$ . We refer below to the “known” relaxation function as “jump1,” while the relaxation function to be compared to the prediction based on jump1 is referred to as “jump2.”

For the times  $t_1^*(R)$  and  $t_2^*(R)$  at which two jumps have the same normalized relaxation function, i.e.,  $R_1 = R_2 = R$ , since  $F(R_1) = F(R_2)$ , Eq. (8) implies that

$$\begin{aligned} -\frac{dR_1}{dt_1^*} \cdot \frac{1}{\gamma_{eq,1}} \cdot \exp\left(-\frac{\Delta\chi(0)_1}{\chi_{const}} R(t_1^*)\right) \\ = -\frac{dR_2}{dt_2^*} \cdot \frac{1}{\gamma_{eq,2}} \cdot \exp\left(-\frac{\Delta\chi(0)_2}{\chi_{const}} R(t_2^*)\right). \end{aligned} \quad (9)$$

If we choose  $dt_1^*$  and  $dt_2^*$  such that  $dR_1 = dR_2$  and use  $R_1(t_1^*) = R_2(t_2^*)$ , Eq. (9) leads to

$$dt_2^* = \frac{\gamma_{eq,1}}{\gamma_{eq,2}} \exp\left(\frac{\Delta\chi(0)_1 - \Delta\chi(0)_2}{\chi_{const}} R(t_1^*)\right) dt_1^*. \quad (10)$$

By integrating this, one gets

$$t_2 = \int_0^{t_2^*} dt_2^* = \frac{\gamma_{eq,1}}{\gamma_{eq,2}} \int_0^{t_1^*} \exp\left(\frac{\Delta\chi(0)_1 - \Delta\chi(0)_2}{\chi_{const}} R(t_1^*)\right) dt_1^*. \quad (11)$$

Equation (11) states that for predicting jump2, one just needs to “transport” the discrete time vector  $\mathbf{t}_1 = (t_1^1, t_1^2, \dots, t_1^n)$  and its corresponding relaxation vector  $\mathbf{R}_1 = (R_1^1, R_1^2, \dots, R_1^n)$  to a new time vector  $\mathbf{t}_2 = (t_2^1, t_2^2, \dots, t_2^n)$ , corresponding to the same  $\mathbf{R}$  vector  $\mathbf{R}_1$ .<sup>40</sup> Thus, by plotting  $(\mathbf{t}_2, \mathbf{R}_1)$  and  $(\mathbf{t}_2, \mathbf{R}_2)$ , data are predicted to collapse if SPA applies. For jumps to the same target temperature, Eq. (11) reduces to<sup>8</sup>

$$t_2 = \int_0^{t_1} \exp\left(\frac{\Delta\chi(0)_1 - \Delta\chi(0)_2}{\chi_{const}} R(t_1^*)\right) dt_1^*. \quad (12)$$

The more general SPA version developed by Roed *et al.*<sup>40</sup> allows one to predict all jumps from the knowledge of a single jump and

TABLE I. Different values of  $\chi_{const}$ —derived using Eq. (14) for jumps from 0.60 and 0.50 to the target temperature 0.55.

Quantity	$U$	$W$	$(\nabla U)^2$	$\nabla^2 U$
$\chi_{const}$	0.018 57	0.099 44	5.117	10.04

$\chi_{const}$  [still assuming that  $\Delta T$  is small enough to justify the first-order Taylor expansion given in Eq. (4)]. In contrast to the first SPA derivation considering only jumps to the same target temperature,<sup>8</sup> however, one needs to know the equilibrium clock rate,  $\gamma_{eq}$ , at the target temperature  $T_0$ . In this paper, we identified this quantity from  $\gamma_{eq} \equiv 1/\tau$ , in which the relaxation time  $\tau$  is determined from the intermediate scattering function evaluated at the wave vector corresponding to the first-peak maximum of the AA particle radial distribution function ( $\tau$  is the time at which this quantity has decayed to 0.2).

From two jumps to the same target temperature, by means of Eq. (12),  $\chi_{const}$  can be determined and subsequently used to predict all the other jumps. Thus, Eq. (12) implies that

$$t_2(R) - t_1(R) = \int_0^{t_1(R)} \left[ \exp\left(\frac{\Delta\chi(0)_1 - \Delta\chi(0)_2}{\chi_{const}} R(t_1^*)\right) - 1 \right] dt_1^*. \quad (13)$$

A similar expression applies for  $t_1(R) - t_2(R)$ . Taking the long-time limits of these expressions for the two normalized relaxation functions in question leads to the self-consistency requirement,<sup>8</sup>

$$\begin{aligned} \int_0^\infty \left[ \exp\left(\frac{\Delta\chi(0)_1 - \Delta\chi(0)_2}{\chi_{const}} R(t_1^*)\right) - 1 \right] dt_1^* \\ + \int_0^\infty \left[ \exp\left(\frac{\Delta\chi(0)_2 - \Delta\chi(0)_1}{\chi_{const}} R(t_2^*)\right) - 1 \right] dt_2^* = 0. \end{aligned} \quad (14)$$

Equation (14) is an equation for  $\chi_{const}$  that is easily solved numerically. The value of  $\chi_{const}$  depends on the quantity probed, of course. Table I provides the values of  $\chi_{const}$  for the four different quantities monitored.

## V. TEMPERATURE-JUMP RESULTS

Figure 3 investigates SPA for jumps to the same target temperature ( $T_0 = 0.55$ ). In the upper panels, down jumps (green) were used to predict up jumps (blue), and in the lower panels, up jumps were used to predict down jumps. The relaxation curves do not start at unity because of the already mentioned “instantaneous” jump that occurs within the first few time steps of an aging simulation. The relative magnitude of this jump depends on the quantity in question. Jumps to different target temperatures were also investigated (Fig. 4). The predictions in the upper panels are based on up jumps, while the predictions in the lower panels are based on down jumps. There are small deviations at the beginning, and the predictions do not fit data as well for larger jumps as for smaller ones. Despite these

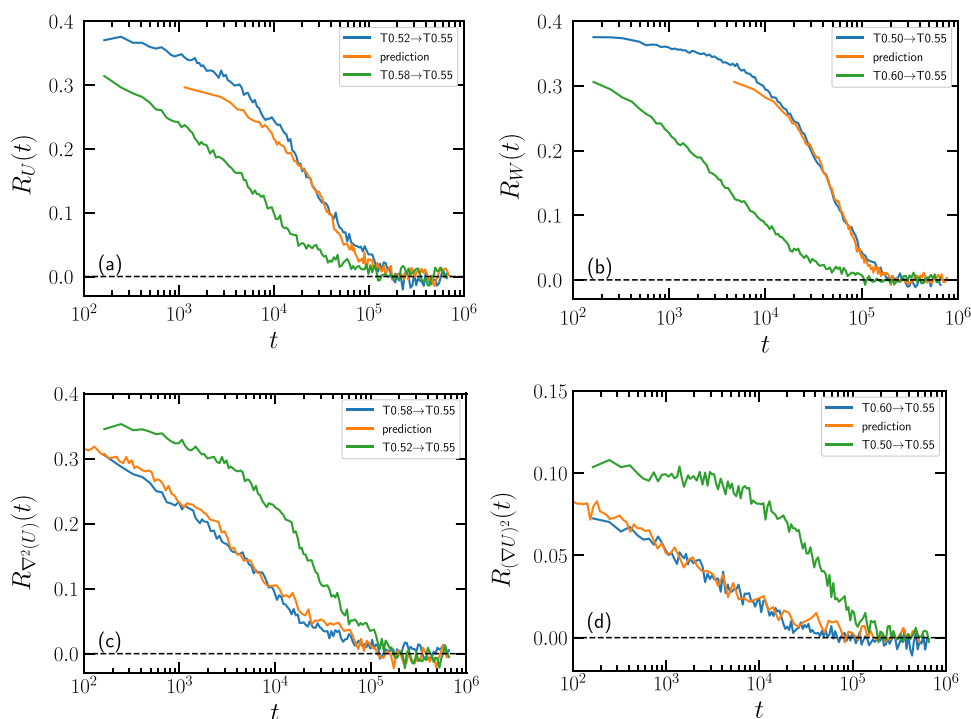


**FIG. 3.** Test of the SPA predictions for jumps to the same target temperature  $T_0 = 0.55$ . The data for the “jump1” normalized relaxation functions  $R(t)$  are represented by the green curves. The predictions based on jump1 according to Eq. (12) are represented by the orange curves. These are to be compared to the “jump2” data (blue curves). (a) and (b) give the predictions of up jumps based on down jumps for the potential energy and the virial, respectively. (c) and (d) give the predictions of down jumps based on up jumps for the Laplacian of the potential energy and the average squared force, respectively.

minor deviations, we conclude that, overall, the results validate SPA for computer simulations.

Figures 5 and 6 plot for each temperature jump all four relaxation curves. The curves have here been scaled empirically by

multiplying  $R(t)$  by a constant in order to be able to compare the relaxing parts of the aging signals. We see that the four quantities relax almost identically. This demonstrates a physically appealing version of SPA according to which all four quantities’ age in

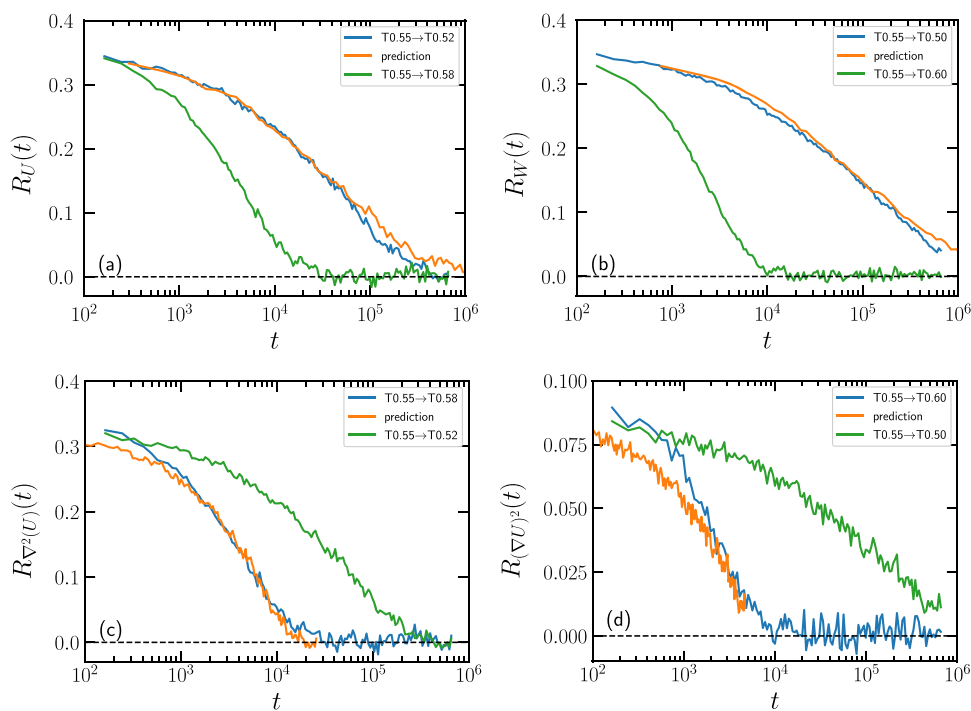


**FIG. 4.** SPA tested for jumps starting at the same temperature (0.55) and ending at different target temperatures. Jump1 data are represented by the green curves. The predictions based on jump1 according to Eq. (12) are represented by orange, while the jump2 simulation results are represented by blue. (a) and (b) give the predictions of down jumps based on up jumps for the potential energy and the virial, respectively. (c) and (d) give the predictions of up jumps based on down jumps for the Laplacian of the potential energy and the average squared force, respectively.

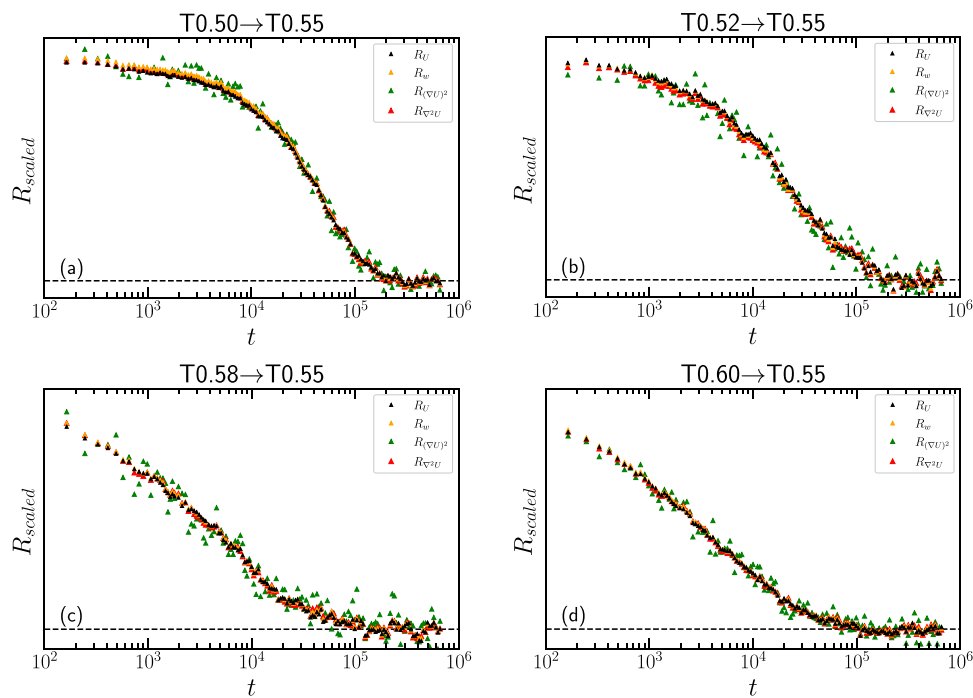


**FIG. 5.** Empirically scaled relaxation curves of the four quantities, plotted for each of the four jumps to the target temperature 0.55. The black points represent the potential energy, yellow points represent the virial, green points represent the average squared force, and red points represent the Laplacian of the potential energy. The dashed lines mark zero.

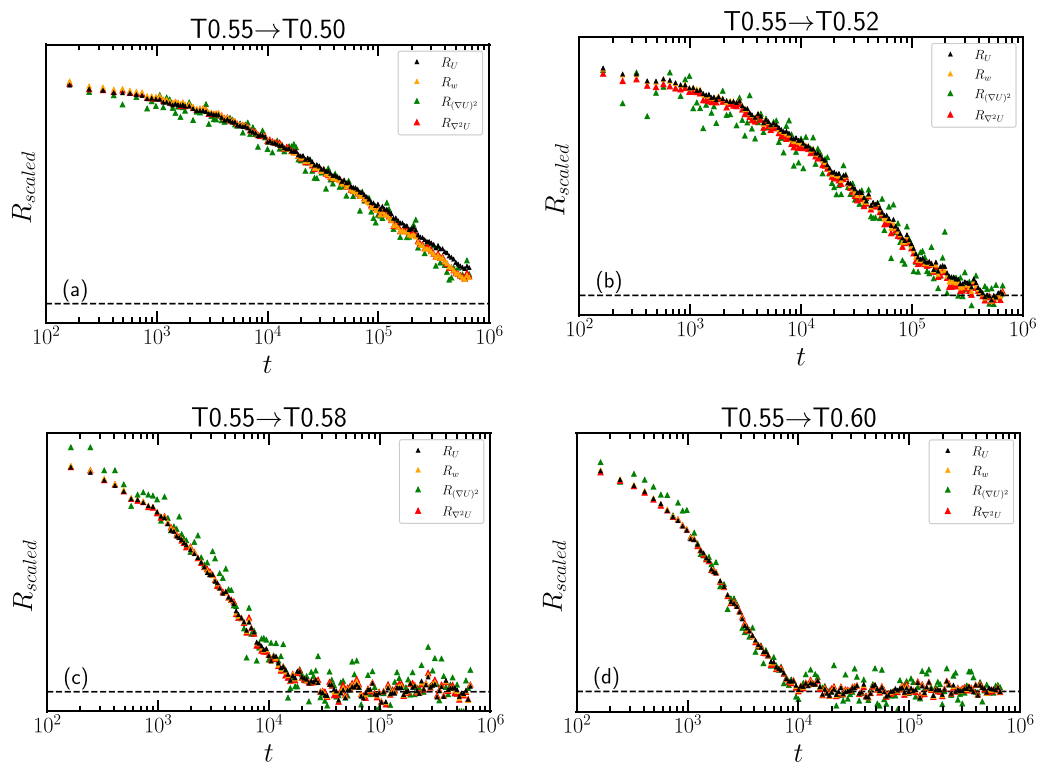


**FIG. 6.** Empirically scaled relaxation curves of the four quantities, plotted for each of the four jumps away from the target temperature 0.55. The same color codes are used here as in Fig. 5.

the same way and controlled by the same material time. This is consistent with a material time thought of physically as reflecting the time on an “internal clock” of the aging system. In the present context, we note, however, that part of the scaled relaxing curves being virtually identical is not surprising. Thus, it is known that binary Lennard-Jones systems have strong virial potential-energy correlations, implying that in equilibrium, the virial is a linear function of the potential energy.<sup>55–57</sup> This extends to out-of-equilibrium situations.<sup>58</sup> Thus, one expects the virial and the potential energy to have the same relaxation functions, except for scaling constants. Likewise, the observation that the configurational temperature equilibrates almost instantaneously implies that its numerator (the average squared force) and its denominator (the Laplacian of the potential energy) must have the same relaxation functions.

## VI. DISCUSSION

While physical aging is usually studied experimentally, computer simulations provide an alternative means for systematically investigating aging. For instance, it is much easier to control and rapidly change temperature in a computer simulation. It should be noted, though, that it is only with the presently available strong computing powers that it is possible to obtain the simulation results of a quality approaching that of the best aging experiments.

We find that SPA works well in computer simulations, albeit with an accuracy that decreases somewhat as the jump size increases. This is not surprising since a first-order Taylor expansion was used to derive SPA. It is important to note, however, that the largest temperature jumps considered here are, relatively, almost ten times larger than those of the experimental validations of the SPA formalism<sup>8,40</sup> (10% vs 1%). Not surprisingly, the larger the deviations observed in some of the predictions at the beginning are, the larger the jumps are. Confirming the previous findings by Powles and co-workers,<sup>54</sup> we find that the configurational temperature,  $k_B T_{\text{conf}}$ , does not age; on the other hand, both its numerator and denominator age following SPA. We recommend using data from up and down jumps with the same magnitude to the same target temperature when identifying  $\chi_{\text{const}}$  by use of Eq. (14). In this way, one avoids the need to model the temperature dependence of  $\gamma_{\text{eq}}$ .

The above-mentioned computer simulations were performed at constant volume. We have not attempted to test SPA in constant-pressure simulations but expect that SPA applies equally well here. Thus, the experiments confirming SPA were all performed at ambient pressure;<sup>8,40</sup> moreover, the SPA derivation does not assume constant-volume conditions.

SPA is the simplest aging scenario consistent with the TN concept of a material time. This is because SPA is derived by assuming just a single relevant parameter and because first-order Taylor expansions are used.<sup>8</sup> Our finding that all four quantities conform to SPA and relax in the same way shows that they are controlled by the same material time. This is not trivial. Whether all quantities of the binary LJ system age controlled by this clock is an interesting question for future work. It would also be interesting to investigate whether the agreement with simulations may be

improved by Taylor expanding to higher order, without making the SPA formalism highly involved or introducing a wealth of adjustable parameters.

## ACKNOWLEDGMENTS

This work was supported by the VILLUM Foundation’s *Matter* Grant (No. 16515).

## DATA AVAILABILITY

The data that support the findings of this study are available from the corresponding author upon reasonable request. We thank Lorenzo Costigliola and Thomas Schröder for technical assistance.

## REFERENCES

- <sup>1</sup>D. Cangialosi, “Dynamics and thermodynamics of polymer glasses,” *J. Phys.: Condens. Matter* **26**, 153101 (2014).
- <sup>2</sup>A. Q. Tool, “Relation between inelastic deformability and thermal expansion of glass in its annealing range,” *J. Am. Ceram. Soc.* **29**, 240–253 (1946).
- <sup>3</sup>O. S. Narayanaswamy, “A model of structural relaxation in glass,” *J. Am. Ceram. Soc.* **54**, 491–498 (1971).
- <sup>4</sup>G. W. Scherer, *Relaxation in Glass and Composites* (Wiley, New York, 1986).
- <sup>5</sup>I. M. Hodge, “Physical aging in polymer glasses,” *Science* **267**, 1945–1947 (1995).
- <sup>6</sup>C. T. Moynihan, A. J. Easteal, M. A. De Bolt, and J. Tucker, “Dependence of the fictive temperature of glass on cooling rate,” *J. Am. Ceram. Soc.* **59**, 12–16 (1976).
- <sup>7</sup>N. B. Olsen, J. C. Dyre, and T. Christensen, “Structural relaxation monitored by instantaneous shear modulus,” *Phys. Rev. Lett.* **81**, 1031 (1998).
- <sup>8</sup>T. Hecksher, N. B. Olsen, and J. C. Dyre, “Communication: Direct tests of single-parameter aging,” *J. Chem. Phys.* **142**, 241103 (2015).
- <sup>9</sup>J. C. Mauro, R. J. Loucks, and P. K. Gupta, “Fictive temperature and the glassy state,” *J. Am. Ceram. Soc.* **92**, 75–86 (2009).
- <sup>10</sup>L. F. Cugliandolo and J. Kurchan, “On the out-of-equilibrium relaxation of the Sherrington-Kirkpatrick model,” *J. Phys. A: Math. Gen.* **27**, 5749 (1994).
- <sup>11</sup>W. Kob and J.-L. Barrat, “Fluctuations, response and aging dynamics in a simple glass-forming liquid out of equilibrium,” *Eur. Phys. J. B* **13**, 319–333 (2000).
- <sup>12</sup>D. B. Adolf, R. S. Chambers, J. Flemming, J. Budzien, and J. McCoy, “Potential energy clock model: Justification and challenging predictions,” *J. Rheol.* **51**, 517–540 (2007).
- <sup>13</sup>H. E. Castillo and A. Parsaeian, “Local fluctuations in the ageing of a simple structural glass,” *Nat. Phys.* **3**, 26–28 (2007).
- <sup>14</sup>A. Parsaeian and H. E. Castillo, “Equilibrium and nonequilibrium fluctuations in a glass-forming liquid,” *Phys. Rev. Lett.* **102**, 055704 (2009).
- <sup>15</sup>I. Kolvin and E. Bouchbinder, “Simple nonlinear equation for structural relaxation in glasses,” *Phys. Rev. E* **86**, 010501 (2012).
- <sup>16</sup>L. C. E. Struik, *Physical Aging in Amorphous Polymers and Other Materials* (Elsevier, Amsterdam, 1978).
- <sup>17</sup>J. M. Hutchinson, “Physical aging of polymers,” *Prog. Polym. Sci.* **20**, 703–760 (1995).
- <sup>18</sup>G. M. Odegard and A. Bandyopadhyay, “Physical aging of epoxy polymers and their composites,” *J. Polym. Sci., Part B: Polym. Phys.* **49**, 1695–1716 (2011).
- <sup>19</sup>D. Cangialosi and V. M. Boucher, A. Alegría, and J. Colmenero, “Physical aging in polymers and polymer nanocomposites: Recent results and open questions,” *Soft Matter* **9**, 8619–8630 (2013).
- <sup>20</sup>L. Grassia and S. L. Simon, “Modeling volume relaxation of amorphous polymers: Modification of the equation for the relaxation time in the KAHR model,” *Polymer* **53**, 3613–3620 (2012).
- <sup>21</sup>J. C. Qiao and J.-M. Pelletier, “Dynamic mechanical relaxation in bulk metallic glasses: A review,” *J. Mater. Sci. Technol.* **30**, 523–545 (2014).

- <sup>22</sup>L. Song, W. Xu, J. Huo, F. Li, L.-M. Wang, M. D. Ediger, and J.-Q. Wang, "Activation entropy as a key factor controlling the memory effect in glasses," *Phys. Rev. Lett.* **125**, 135501 (2020).
- <sup>23</sup>L. Lundgren, P. Svedlindh, P. Nordblad, and O. Beckman, "Dynamics of the relaxation-time spectrum in a CuMn spin-glass," *Phys. Rev. Lett.* **51**, 911 (1983).
- <sup>24</sup>L. Berthier and J.-P. Bouchaud, "Geometrical aspects of aging and rejuvenation in the Ising spin glass: A numerical study," *Phys. Rev. B* **66**, 054404 (2002).
- <sup>25</sup>S. Spinner and A. Napolitano, "Further studies in the annealing of a borosilicate glass," *J. Res. Natl. Bur. Stand., Sect. A* **70A**, 147 (1966).
- <sup>26</sup>E. Schlosser and A. Schönhals, "Dielectric relaxation during physical ageing," *Polymer* **32**, 2135–2140 (1991).
- <sup>27</sup>R. L. Leheny and S. R. Nagel, "Frequency-domain study of physical aging in a simple liquid," *Phys. Rev. B* **57**, 5154 (1998).
- <sup>28</sup>P. Lunkenheimer, R. Wehn, U. Schneider, and A. Loidl, "Glassy aging dynamics," *Phys. Rev. Lett.* **95**, 055702 (2005).
- <sup>29</sup>R. Richert, "Supercooled liquids and glasses by dielectric relaxation spectroscopy," *Adv. Chem. Phys.* **156**, 101–195 (2015).
- <sup>30</sup>T. Hecksher, N. B. Olsen, K. Niss, and J. C. Dyre, "Physical aging of molecular glasses studied by a device allowing for rapid thermal equilibration," *J. Chem. Phys.* **133**, 174514 (2010).
- <sup>31</sup>R. Wehn, P. Lunkenheimer, and A. Loidl, "Broadband dielectric spectroscopy and aging of glass formers," *J. Non-Cryst. Solids* **353**, 3862–3870 (2007).
- <sup>32</sup>J. C. Dyre and N. B. Olsen, "Minimal model for beta relaxation in viscous liquids," *Phys. Rev. Lett.* **91**, 155703 (2003).
- <sup>33</sup>A. J. Kovacs, "Transition vitreuse dans les polymeres amorphes. Etude phenomenologique," *Fortschr. Hochpolym.-Forsch.* **3**, 394–507 (1963).
- <sup>34</sup>X. Di, K. Z. Win, G. B. McKenna, T. Narita, F. Lequeux, S. R. Pullella, and Z. Cheng, "Signatures of structural recovery in colloidal glasses," *Phys. Rev. Lett.* **106**, 095701 (2011).
- <sup>35</sup>G. B. McKenna and S. L. Simon, "50th anniversary perspective: Challenges in the dynamics and kinetics of glass-forming polymers," *Macromolecules* **50**, 6333–6361 (2017).
- <sup>36</sup>O. V. Mazurin, "Relaxation phenomena in glass," *J. Non-Cryst. Solids* **25**, 129–169 (1977).
- <sup>37</sup>G. B. McKenna, "On the physics required for prediction of long term performance of polymers and their composites," *J. Res. Natl. Inst. Stand. Technol.* **99**, 169 (1994).
- <sup>38</sup>I. M. Hodge, "Enthalpy relaxation and recovery in amorphous materials," *J. Non-Cryst. Solids* **169**, 211–266 (1994).
- <sup>39</sup>I. Avramov, "Kinetics of structural relaxation of glass-forming melts," *Thermochim. Acta* **280–281**, 363–382 (1996).
- <sup>40</sup>L. A. Roed, T. Hecksher, J. C. Dyre, and K. Niss, "Generalized single-parameter aging tests and their application to glycerol," *J. Chem. Phys.* **150**, 044501 (2019).
- <sup>41</sup>J. C. Dyre, "The glass transition and elastic models of glass-forming liquids," *Rev. Mod. Phys.* **78**, 953–972 (2006).
- <sup>42</sup>H. N. Ritland, "Limitations of the fictive temperature concept," *J. Am. Ceram. Soc.* **39**, 403–406 (1956).
- <sup>43</sup>J. C. Dyre, "Narayanaswamy's 1971 aging theory and material time," *J. Chem. Phys.* **143**, 114507 (2015).
- <sup>44</sup>W. Kob and H. C. Andersen, "Testing mode-coupling theory for a supercooled binary Lennard-Jones mixture I: The van Hove correlation function," *Phys. Rev. E* **51**, 4626–4641 (1995).
- <sup>45</sup>K. Vollmayr, W. Kob, and K. Binder, "How do the properties of a glass depend on the cooling rate? A computer simulation study of a Lennard-Jones system," *J. Chem. Phys.* **105**, 4714–4728 (1996).
- <sup>46</sup>A. Parsaeian and H. E. Castillo, "Growth of spatial correlations in the aging of a simple structural glass," *Phys. Rev. E* **78**, 060105 (2008).
- <sup>47</sup>C. Rehwal, N. Gnan, A. Heuer, T. Schröder, J. C. Dyre, and G. Diezemann, "Aging effects manifested in the potential-energy landscape of a model glass former," *Phys. Rev. E* **82**, 021503 (2010).
- <sup>48</sup>N. Gnan, C. Maggi, G. Parisi, and F. Sciortino, "Generalized fluctuation-dissipation relation and effective temperature upon heating a deeply supercooled liquid," *Phys. Rev. Lett.* **110**, 035701 (2013).
- <sup>49</sup>N. V. Priezjev, "Slow relaxation dynamics in binary glasses during stress-controlled, tension-compression cyclic loading," *Comput. Mater. Sci.* **153**, 235–240 (2018).
- <sup>50</sup>T. S. Ingebrigtsen, J. C. Dyre, T. B. Schröder, and C. Patrick Royall, "Crystallization instability in glass-forming mixtures," *Phys. Rev. X* **9**, 031016 (2019).
- <sup>51</sup>U. R. Pedersen, T. B. Schröder, and J. C. Dyre, "Phase diagram of Kob-Andersen-type binary Lennard-Jones mixtures," *Phys. Rev. Lett.* **120**, 165501 (2018).
- <sup>52</sup>I. H. Bell, J. C. Dyre, and T. S. Ingebrigtsen, "Excess-entropy scaling in supercooled binary mixtures," *Nat. Commun.* **11**, 4300 (2020).
- <sup>53</sup>T. B. Schröder and J. C. Dyre, "Solid-like mean-square displacement in glass-forming liquids," *J. Chem. Phys.* **152**, 141101 (2020).
- <sup>54</sup>J. G. Powles, G. Rickayzen, and D. M. Heyes, "Temperatures: Old, new and middle aged," *Mol. Phys.* **103**, 1361–1373 (2005).
- <sup>55</sup>N. Gnan, T. B. Schröder, U. R. Pedersen, N. P. Bailey, and J. C. Dyre, "Pressure-energy correlations in liquids. IV. 'Isomorphs' in liquid phase diagrams," *J. Chem. Phys.* **131**, 234504 (2009).
- <sup>56</sup>L. Böhling, T. S. Ingebrigtsen, A. Grzybowski, M. Paluch, J. C. Dyre, and T. B. Schröder, "Scaling of viscous dynamics in simple liquids: Theory, simulation and experiment," *New J. Phys.* **14**, 113035 (2012).
- <sup>57</sup>T. S. Ingebrigtsen and H. Tanaka, "Effect of size polydispersity on the nature of Lennard-Jones liquids," *J. Phys. Chem. B* **119**, 11052–11062 (2015).
- <sup>58</sup>T. B. Schröder, N. P. Bailey, U. R. Pedersen, N. Gnan, and J. C. Dyre, "Pressure-energy correlations in liquids. III. Statistical mechanics and thermodynamics of liquids with hidden scale invariance," *J. Chem. Phys.* **131**, 234503 (2009).